Ccm1 is required for arterial morphogenesis: implications for the etiology of human cavernous malformations

Kevin J. Whitehead[1,2,*], Nicholas W. Plummer[3,*], Jennifer A. Adams[1], Douglas A. Marchuk[3,†] and Dean Y. Li[1,2,†]

[1]Program in Human Molecular Biology and Genetics, University of Utah, Building 533 Room 4220, 15 N 2030 East, Salt Lake City, Utah 84112, USA
[2]Department of Medicine, University of Utah, 4C104 SOM, 30 N 1900 East, Salt Lake City, Utah 84132, USA
[3]Department of Molecular Genetics and Microbiology, Duke University Medical Center, 268 CARL Building, Box 3175, Durham, North Carolina 27710, USA

*These authors contributed equally to this work
†Authors for correspondence (e-mail: march004@mc.duke.edu or dean.li@hmbg.utah.edu)

Accepted 2 December 2003

Development 131, 1437-1448
Published by The Company of Biologists 2004
doi:10.1242/dev.01036

Summary

Hemorrhagic stroke is a significant cause of morbidity and mortality in children, and is frequently associated with intracranial vascular malformations. One prevalent form of these vascular malformations, cerebral cavernous malformation, is characterized by thin-walled vascular cavities that hemorrhage and has been linked to loss-of-function mutations in *CCM1*. The neural and epithelial expression of *CCM1* in adulthood suggests that cavernous malformations may be the result of primary neural defects. In this study, we generated mice lacking *Ccm1* and demonstrate that *Ccm1* is ubiquitously expressed early in embryogenesis and is essential for vascular development. Homozygous mutant embryos die in mid-gestation and the first detectable defects are exclusively vascular in nature. The precursor vessels of the brain become dilated starting at E8.5, reminiscent of the intracranial vascular defects observed in the human disease. In addition, there is marked enlargement and increased endothelial proliferation of the caudal dorsal aorta, as well as variable narrowing of the branchial arch arteries and proximal dorsal aorta. These vascular defects are not secondary to primary neural defects, as neural morphology and marker expression are normal even subsequent to the onset of vascular pathology. The defects in the vascular structure of embryos lacking *Ccm1* are associated with early downregulation of artery-specific markers, including the *Efnb2*- and *Notch*-related genes. Finally, consistent with the murine data, we found that there is an analogous reduction in *Notch* gene expression in arterioles from humans with mutations in *CCM1*. Our studies suggest that cavernous malformations result from primary vascular rather than neural defects.

Supplemental data available online

Key words: Ccm1, Gene targeting, Mice, Angiogenesis, Stroke, Epilepsy, Notch, Efnb2

Introduction

Stroke is an important cause of morbidity and mortality in children where it ranks in the top 10 causes of death (Arias and Smith, 2003; Lynch et al., 2002). Approximately 20% of pediatric stroke cases are due to intracranial hemorrhage, the most common underlying cause of which is vascular malformations (Lynch et al., 2002). Cerebral cavernous malformations (CCM) represent an important subset of such vascular malformations. They are common, being found in 0.5% of the population in autopsy and MRI surveillance studies (Del Curling et al., 1991; Otten et al., 1989; Robinson et al., 1991). These lesions are classically defined by enlarged and thin-walled vascular structures in the central nervous system (CNS) without intervening brain parenchyma, lined by endothelial cells and lacking supporting vascular smooth muscle cells.

Recently it has been shown that a monogenic form of CCM is linked to loss-of-function mutations in the *CCM1* locus on chromosome 7q, which encodes the KRIT1 protein (Craig et al., 1998; Laberge-le Couteulx et al., 1999; Marchuk et al., 1995; Moriarity et al., 1999; Rigamonti et al., 1988; Sahoo et al., 1999). KRIT1 is an intracellular protein with ankyrin repeats and a FERM domain (Serebriiskii et al., 1997; Zawistowski et al., 2002), initially cloned on the basis of a yeast two-hybrid interaction with KREV1/RAP1a, a small RAS family GTPase (Serebriiskii et al., 1997). Subsequently, additional 5′ sequences were found that extend the open reading frame (Sahoo et al., 2001; Zhang et al., 2000). The longer protein did not interact with KREV1/RAP1a, but instead showed strong interaction with integrin cytoplasmic domain associated protein-1-alpha (ICAP1α) (Faisst and Gruss, 1998; Zawistowski et al., 2002; Zhang et al., 2001), which binds a similar NPXY motif on both KRIT1 and β1-integrin (Zawistowski et al., 2002; Zhang et al., 2001). In addition, KRIT1 interacts with the plus ends of microtubules, suggesting a possible role in microtubule targeting (Gunel et al., 2002). Although these biochemical data have provided

useful insights into KRIT1 function in vitro, the in vivo role of KRIT1 remains unclear, particularly with respect to vascular disease.

Using in situ hybridization, others have reported that *Ccm1* is expressed ubiquitously until E10.5, at which point the expression starts to become restricted to neural and epithelial tissues (Denier et al., 2002; Kehrer-Sawatzki et al., 2002). These studies suggest that *Ccm1* may play a role in neural development or function, and have led some authors to suggest that *Ccm1* does not play a role in cardiovascular development (Kehrer-Sawatzki et al., 2002). The neural and epithelial expression of *Ccm1* in adulthood suggests that cavernous malformations may be the result of primary neural defects.

Human vascular malformation syndromes, such as CCM, affect the junction between veins and arteries. Arteries and veins form separately but follow parallel trajectories and can be distinguished on the basis of molecular markers, even prior to the onset of flow at E8.5 (Ji et al., 2003; McGrath et al., 2003; Wang et al., 1998). Recent studies in zebrafish have demonstrated a genetic pathway governing arterial identity, in which the expression of *vascular endothelial growth factor* (*Vegf*) is necessary for the expression of arterial markers and morphology (Lawson et al., 2002). Specifically, *Vegf* is necessary for the expression of *Notch* family members in arteries, and *Notch* signaling, in turn, is required for the arterial expression of *ephrin B2* (*Efnb2*) and correct arterial-venous relationships (Lawson et al., 2001). A specific role for this genetic pathway in arterial identity has not yet been confirmed in mammalian systems.

The expanding link between human vascular disorders such as hereditary hemorrhagic telangiectasia (Li et al., 1999; Park et al., 2003; Sorensen et al., 2003; Urness et al., 2000) and CADASIL (Gridley, 2001; Joutel et al., 1996) to molecular pathways implicated in arterial identity and vascular patterning suggests that *Ccm1* may have an essential role in arterial development. Here we demonstrate, using murine gene targeting, that *Ccm1* is required for vascular development. Our data indicate that Krit1-associated vascular defects are not secondary to disrupted neural patterning. We also demonstrate impaired arterial identity in embryos lacking *Ccm1*, and provide evidence that Krit1 lies upstream of Notch signaling in the vasculature in mice and humans. Our studies suggest that mutations in *Ccm1* impact vascular development and disease by disrupting a genetic pathway important in establishing arterial identity.

Materials and methods

Targeted deletion of *Ccm1*

We designed a construct to delete the first ankyrin repeat of *Ccm1* by replacing most of coding exon 6 and all of exon 7 with an internal ribosomal entry site and the *E. coli lacZ* gene. Genomic fragments of 2.0 kb and 4.5 kb from the 5′ and 3′ ends of the targeted region, respectively, were cloned into the pPNT vector (Tybulewicz et al., 1991), together with the IRES-*lacZ* gene from plasmid pENβ16-B (both plasmids were a gift from Dr Yuan Zhuang). Transfected R1 embryonic stem cells were screened for correct integration of the targeting vector by PCR and sequencing, as well as by Southern blotting. A founder that transmitted the *Ccm1*^{tm1Dmar} allele to its progeny was obtained. Mouse genotypes were determined by PCR (Barrow et al., 2003) using allele-specific primers (sequences available upon request). Mice heterozygous for the allele were backcrossed for at least five generations to C57BL/6J mice.

In situ hybridization

We carried out in situ hybridization at 70°C as previously described (Urness et al., 2000). Probes were generated by in vitro transcription of appropriate plasmids. We were provided plasmids for *Hand1*, *Hand2* (Dr Deepak Srivastava), *Dll4* (Dr John Shutter, Amgen), *Notch4* (Dr Thomas Gridley) and *Efnb2* (Dr David Anderson). Using RT PCR on mouse cDNA with appropriate primers (sequences available upon request) we generated probe templates for *Ccm1*, *IRES-lacZ*, *Nppa*, *Six3*, *Otx2*, *Fgf8*, *Gbx2*, *Shh*, *Pax7*, *Nkx2-2*, *Ntn1*, *Brachyury* and *Vegfa*. A probe for *MafB* was generated by in vitro transcription of an EST (IMAGE: 2811217).

Immunohistochemistry

Mouse tissues were studied with antibodies to Pecam (clone MEC13.3, BD Biosciences) and α-smc actin (clone 1A4, DAKO). Human tissues were studied with antibodies to PECAM (clone JC70A, DAKO) and NOTCH4 (polyclonal H-225, SantaCruz).

In vivo proliferation and apoptosis

Frozen sections were stained first with Pecam antibody (clone MEC13.3, BD Biosciences), followed by antibodies against phospho-histone H3 or cleaved caspase 3 (Cell Signaling Technology). Finally, appropriate fluorescent secondary antibodies (Jackson ImmunoResearch) were applied. Slides were counterstained with DAPI (Molecular Probes).

Total endothelial nuclei and mitotic endothelial nuclei were counted from the dorsal aorta, branchial arch arteries, and vitelline arteries, and data were labeled as originating from either caudal or rostral regions. All sections distal to the sinus venosus of the heart were considered caudal. The mean percentages of rostral or caudal mitotic nuclei for each of three separate experiments were compared using an unpaired *t*-test (InStat, by GraphPad software).

Confocal immunofluorescence

Embryos were prepared for confocal immunofluorescent detection of PECAM antigen as previously described (Drake and Fleming, 2000). Images were obtained using an Olympus FluoView™ 300 confocal microscope (University of Utah Cell Imaging Core).

India ink injection

Ink injections were carried out in E8.5-E9.5 embryos as previously described (Urness et al., 2000). Following ink injection, yolk sacs were removed and embryos were photographed directly.

β-Galactosidase staining

Mice heterozygous for *Efnb2* expressing a *tau-lacZ* transgene under the control of the *Efnb2* locus were previously generated and described (Wang et al., 1998). We crossed this transgene into *Ccm1* heterozygous mice. Double heterozygous (both *Ccm1* and *Efnb2*) male mice were mated with *Ccm1* heterozygous females to generate embryos heterozygous for *Efnb2* with all possible *Ccm1* genotypes. Genotyping was performed with allele-specific primers (sequences available upon request). Staining for β-galactosidase expression was performed with X-gal as previously described (Sorensen et al., 2003). Littermates homozygous for *Ccm1* and wild type at the *Efnb2* locus were used to control for the negligible embryonic β-galactosidase expression from the *Ccm1 IRES-lacZ* construct.

Real-time quantitative RT-PCR

RNA was isolated from single E8.8 (13 somite) embryos (RNAqueous 4PCR kit, Ambion) and used as template to make random primed cDNA (RetroScript kit, Ambion). Assays for *Efnb2*, *Dll4*, *Notch4* and *Vegfa* were obtained, as well as for *Ccm1* as a control for genotype (Assays-on-Demand, Applied Biosystems), and used according to the

manufacturer's instructions on an Applied Biosystems 7900HT thermal cycler (University of Utah Genomics Core Facility). Transcripts were normalized in relation to *Gapdh* expression (rodent GAPDH, Applied Biosystems). Comparisons were made between three separate pairs of wild-type and homozygous mutant embryos, and reported in relation to wild-type expression (samples run in triplicate).

Results

Mice lacking *Ccm1* phenocopy human CCM

To explore the role of *Ccm1* in vascular development, we generated a *Ccm1* mutant allele (*Ccm1*^{tm1Dmar}) by disrupting the gene at the first ankyrin repeat with our targeting vector (Fig. 1A-C). At E8.5, no *Ccm1* expression was detected in homozygous mutant mice, although we observed ubiquitous *Ccm1* transcript expression in wild type (Fig. 1D), similar to previous reports (Denier et al., 2002; Kehrer-Sawatzki et al., 2002). Heterozygous mutant mice were phenotypically normal on the C57BL/6J genetic background. Homozygous mutant embryos were grossly indistinguishable from their littermates prior to E9.0. Mutant embryos suffered from generalized developmental arrest after E9.5, and retained a primitive yolk sac vascular network, failed to complete turning, and developed pericardial effusions and atrial enlargement. *Ccm1*^{tm1Dmar}/*Ccm1*^{tm1Dmar} embryos (hereafter referred to as *Ccm1*$^{-/-}$) were disintegrating by E10.0 and no embryos survived beyond E11.0.

Defective development in *Ccm1*$^{-/-}$ embryos was first observed in the vascular system. From E8.5-E9.5, the vessels of the cephalic mesenchyme became progressively dilated (Fig. 2A-D). These vessels will invade the neural tube and start to form the intracranial vascular network at E10.0 (Ruhrberg et al., 2002), a stage in development that *Ccm1*$^{-/-}$ embryos fail to reach. The dilatation in the precursor vessels of the brain is reminiscent of the dilated endothelial sacs observed in the intracranial vasculature of patients with functional hemizygosity at the *CCM1* locus (Fig. 2E,F).

The initial developmental defects in *Ccm1*$^{-/-}$ mice are vascular

To determine developmental defects that could be directly attributed to *Ccm1*, we searched for the earliest histologic and morphologic defects in mice lacking *Ccm1*. We observed vascular dilatation starting at E8.5. In a cross-sectional survey through multiple developmental stages, staining for Pecam revealed ectatic vessels in the embryo (Fig. 3A-D). Dilatation occurred throughout the aorta just distal to the heart and extended to the most caudal regions of the embryo. Shortly after their formation between E8.5 and E9.0, the intersomitic arteries of the embryo also enlarge (data not shown). We observed no enlargement of the adjacent cardinal veins, and no evidence of arteriovenous shunts. Thus, loss of *Ccm1* leads to arterial dilatation that begins after the axial vascular pattern has been established by vasculogenesis.

We sought to determine whether this aortic enlargement was attributable to increased endothelial proliferation or decreased apoptosis. We assessed proliferation by double immunolabeling embryos with antibodies against Pecam and phosphorylated histone 3 (H3P), a specific marker of the mitotic phase of the cell cycle (Brenner et al., 2003; Hendzel et al., 1997; Nechiporuk and Keating, 2002). We observed a twofold

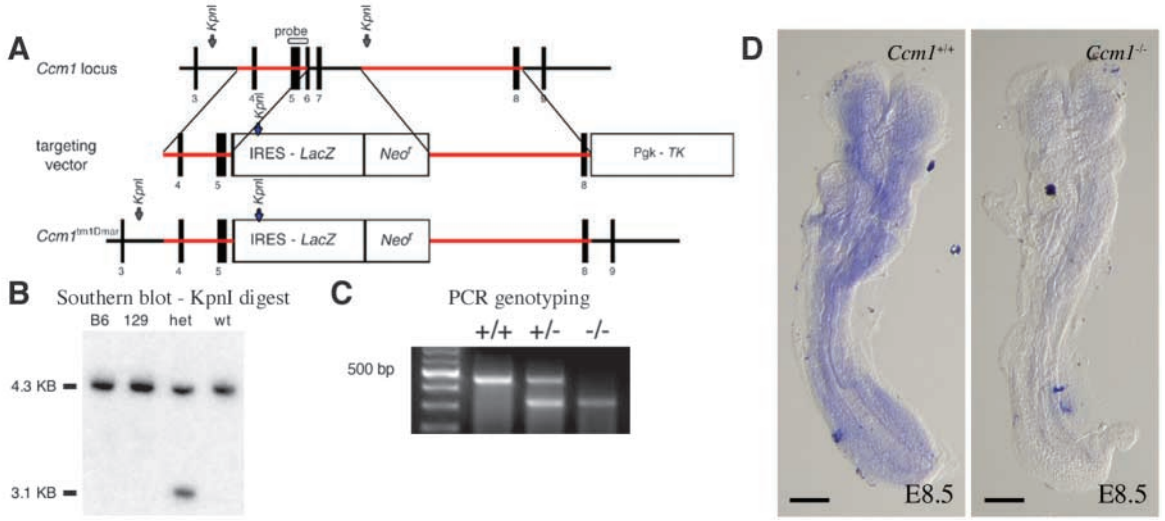

Fig. 1. Generation of mice lacking *Ccm1*. (A) Targeting strategy to generate the *Ccm1*^{tm1Dmar} allele. Mice heterozygous for the allele will be referred to as *Ccm1*$^{+/-}$, and mice homozygous for the allele will be referred to as *Ccm1*$^{-/-}$. Our construct was designed to replace most of the sixth and the entire seventh coding exon of mouse *Ccm1* with an internal ribosomal entry site (IRES) and the *E. coli lacZ* gene. Although this construct successfully ablated *Ccm1* gene expression, we were unable to detect any β-galactosidase protein or enzyme activity in *Ccm1*$^{+/-}$ or *Ccm1*$^{-/-}$ embryos. (B) Southern blotting of *Kpn*I-digested genomic DNA detects a 3.1 kb band from the recombinant allele of a heterozygous animal. This same probe detects a 4.3 kb band from the parent strains (C57BL/6J, labeled B6, and 129X1Sv/J, labeled 129), from the wild-type allele of a heterozygous animal and from a wild-type littermate. Long-range PCR and sequencing of the resulting product also confirmed homologous recombination and conserved sequence at the 3′ and 5′ ends. (C) Genotyping of mice was performed using allele specific PCR primers. The wild-type primers amplify a 466 bp product, and the mutant primers amplify a 310 bp product. (D) In situ hybridization for *Ccm1* detects ubiquitous expression at E8.5 in a wild-type embryo. No transcript is detected in *Ccm1*$^{-/-}$ embryos using this probe, which spans exons 3 through 7. Scale bars: 200 μm.

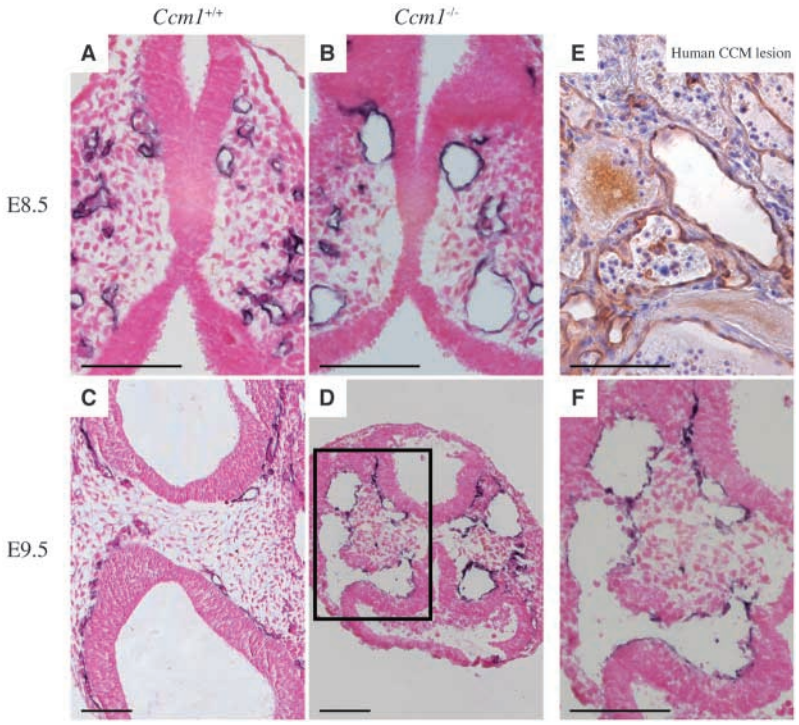

Fig. 2. Dilated cranial vessels in *Ccm1*$^{-/-}$ mice phenocopy human cavernous malformations. (A-D) Immunohistochemical staining for the endothelial antigen Pecam on cross-sections from cranial portions of the embryo. (A,B) Immunostaining reveals the plexus of head vessels at E8.5. Significant enlargement of cranial vessels is observed early in *Ccm1*$^{-/-}$ embryos (B). (C,D) Examination of embryos at E9.5 shows further enlargement of cranial vessels in *Ccm1*$^{-/-}$ embryos, which now occupy much of the region normally encompassed by mesenchymal tissue. By this stage, *Ccm1*$^{-/-}$ mice are readily distinguished from their phenotypically normal littermates and no further embryonic enlargement is observed. (E,F) Comparison of a human cavernous malformation (E) with a similar magnification of a *Ccm1*$^{-/-}$ mouse embryo (F) shows cavernous vascular channels surrounded by a thin layer of Pecam-stained endothelium (stained brown). Human lesions contain vessels of widely varying sizes, some larger than those shown. Scale bars: 100 μm.

increase in mitotic endothelial cells from the dilated distal aortae in *Ccm1*$^{-/-}$ embryos, as compared with wild-type controls (Fig. 3E-G). There were no differences in H3P staining of more rostral regions of the *Ccm1*$^{-/-}$ aortae and branchial arch arteries compared with wild-type controls. There was also no difference in vascular apoptosis observed in *Ccm1*$^{-/-}$ embryos, as assessed by immunofluorescence using antibodies against cleaved Caspase 3. Thus, mice lacking *Ccm1* show extensive vascular dilatation following vasculogenesis associated with an increased endothelial proliferative rate.

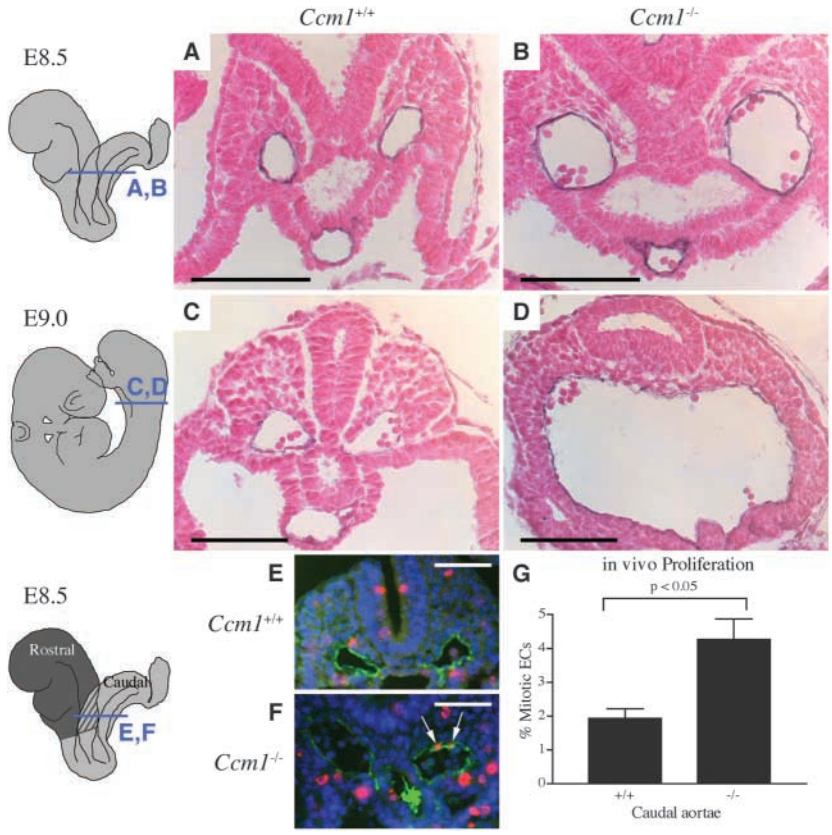

Fig. 3. Vascular dilatation in mice lacking *Ccm1*. (A-D) Immunohistochemical stains for the endothelial antigen Pecam on cross-sections taken from caudal regions of the embryo (as indicated in diagrams to the left). (A,B) The paired dorsal aortae and midline vitelline arteries are apparent at E8.5. Significant enlargement is observed in the dorsal aortae of *Ccm1*$^{-/-}$ embryos. (C,D) A comparison of wild-type (C) and *Ccm1*$^{-/-}$ (D) embryos at E9.0. There is marked enlargement and midline fusion of the dorsal aortae in the *Ccm1*$^{-/-}$ embryo. The enlarged vessel occupies almost the entire volume of the embryo and distorts the closed neural tube. (E-G**)** Endothelial proliferation at E8.5 in vivo as determined by immunofluorescent double-labeling with antibodies for Pecam and phosphorylated histone 3, a marker of mitosis. Sections were counterstained with DAPI to define cell nuclei. (E,F) Sections taken from wild-type and homozygous mutant embryos, respectively. Two double-positive (mitotic) endothelial nuclei are demonstrated in the *Ccm1*$^{-/-}$ embryo (arrows in F). (G) A significantly increased endothelial cell proliferative rate is observed for the dilated aortae of *Ccm1*$^{-/-}$ embryos, distal to the heart (light gray portion of embryo diagram to left). Proliferative rates from more rostral sections of aorta and branchial arch arteries were similar between *Ccm1*$^{+/+}$ and *Ccm1*$^{-/-}$ embryos. Data bars represent the mean values from three separate embryo pairings, and a total of 137 *Ccm1*$^{+/+}$ and 192 *Ccm1*$^{-/-}$ aortic cross-sections. Error bars represent s.e.m. Scale bars: 100 μm.

To obtain a more complete view of the vasculature, we performed whole-mount confocal immunofluorescence using Pecam antibodies (Fig. 4A-D). The enlargement of the distal dorsal aortae was again observed (arrow in Fig. 4B); however, in contrast to the extensive vascular dilatation, we observed a discrete region of vascular narrowing in the first branchial arch artery and adjacent proximal dorsal aorta that develops at E8.5 (Fig. 4D). All *Ccm1*$^{-/-}$ embryos at E8.5 have this narrowing; however, the extent and severity of involvement is variable.

To understand the effects that *Ccm1*$^{-/-}$ vascular defects have on circulation, we performed India ink microangiography. Injection of India ink into the ventricle of an E8.5 heart filled the first branchial arch artery and entire dorsal aorta of the wild-type embryo (Fig. 4E). By contrast, no ink passed through the branchial arch arteries of *Ccm1*$^{-/-}$ embryos and the dilated portions of the dorsal aorta were not opacified (Fig. 4F). Similar observations were made at E9.5, at which point the normal passage of ink is through the second and third pairs of branchial arch arteries (Fig. 4G). A small amount of ink was observed in the narrowed first and second branchial arch arteries of *Ccm1*$^{-/-}$ embryos, with minimal filling of the adjacent dorsal aorta. The dilated vascular malformation of the caudal embryo was not seen angiographically (Fig. 4H). This is analogous to human CCM lesions, which are typically not observed on cerebral angiography (Robinson et al., 1993), implying that such lesions may also have narrowed arterial inflow.

We further characterized the time-course of this narrowing with a developmental series of embryo cross-sections stained for Pecam. These studies indicated that the proximal aorta and the first branchial arch artery formed normally at E8.0 (Fig. 5A,B). At E8.5, the first branchial arch artery had failed to enlarge (Fig. 5C,D). At E9.0, the vestige of the first arch artery and adjacent aorta remained severely narrowed (Fig. 5E,F), and the formation of the second branchial arch artery was abnormal (Fig. 4G,H; and data not shown). We postulated that this narrowing might be due to increased vascular apoptosis, yet we

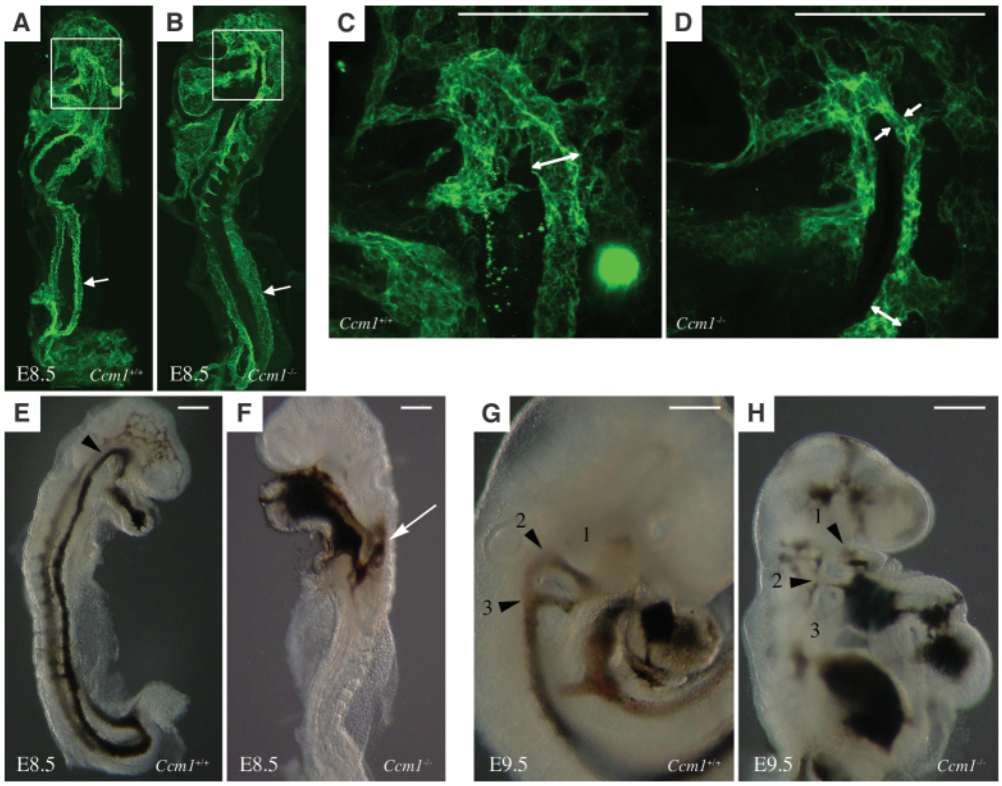

Fig. 4. Proximal narrowing limits flow into dilated distal vessels of *Ccm1*$^{-/-}$ mice. (A-D) Confocal immunofluorescent detection of the endothelial antigen Pecam. (A,B) Composite whole-mount images of E8.5 *Ccm1*$^{+/+}$ and *Ccm1*$^{-/-}$ embryos. The amnion and yolk sac have been removed, allowing the embryos to be extended (some kinking of the midpoint of the *Ccm1*$^{+/+}$ embryo resulted). Note the enlarged diameter of the dorsal aorta of the caudal *Ccm1*$^{-/-}$ embryo (arrow in B). The intersomitic arteries that extend dorsally from the aorta are dilated and more prominent in *Ccm1*$^{-/-}$ embryos. (C,D) Higher magnification views of the first branchial arch artery and proximal aorta (see boxes in A and B). The wild-type embryo has a uniform, broad dorsal aorta (double arrow in C). By contrast, the *Ccm1*$^{-/-}$ embryo shows narrowing of the branchial arch artery and adjacent dorsal aorta (single arrows in D). Distally, the aorta restores to a more normal diameter (double arrow in D). (E-H) Injection of India ink into the ventricle of embryonic hearts. (E,F) At E8.5, ink fills the first branchial arch artery and dorsal aorta of a wild-type embryo, eventually entering the head veins. Ink fails to enter the dorsal aorta of a *Ccm1*$^{-/-}$ embryo, and instead flows in a retrograde manner through the sinus venosus and into the common cardinal vein (arrow in F). Yolk sacs were removed following injection to improve visualization. (G,H) At E9.5, injected ink flows primarily through the second and third branchial arch arteries to fill the dorsal aorta (arrowheads in G). Ink also fills the venous system of the embryo. By contrast, injection of a *Ccm1*$^{-/-}$ embryo fails to opacify the dorsal aorta. A small amount of ink is observed in the first and second branchial arch arteries (arrowheads in H) with a minimal amount entering the adjacent aorta. Scale bars: 200 μm.

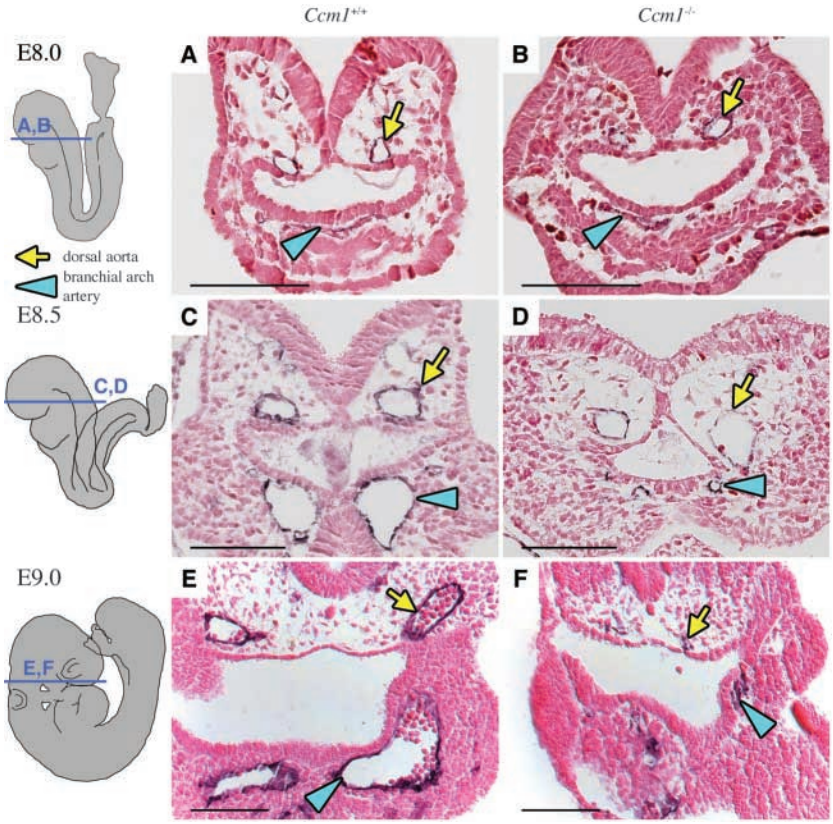

Fig. 5. Branchial arch arteries and adjacent dorsal aortae become narrowed in mice lacking *Ccm1*. (A-F) Immunohistochemical stains for the endothelial antigen Pecam on sagittal sections of embryos. Yellow arrows indicate one of the paired dorsal aortae; blue arrowheads highlight one of the paired branchial arch arteries. (A,B) No differences are observed between $Ccm1^{+/+}$ and $Ccm1^{-/-}$ embryos at E8.0. A patent lumen is present in the bilateral dorsal aortae. A cord of endothelial tissue extends bilaterally from the aortic sac, through the branchial arch towards the dorsal aortae. (C,D) At E8.5, the $Ccm1^{+/+}$ embryo has formed a widely patent first branchial arch artery, whereas the branchial arch arteries of the $Ccm1^{-/-}$ embryo fail to enlarge. (E,F) Further enlargement of these vessels is present at E9.0 in a wild-type embryo. The $Ccm1^{-/-}$ embryo, however, is left with only a vestige of the branchial arch arteries and dorsal aortae. Scale bars: 100 μm.

found no immunological evidence of increased cell death at E8.5 (data not shown). We also did not observe differential endothelial proliferation by immunostaining against phosphorylated histone H3 in this discrete region of the embryo, although this method may lack sufficient power to detect a difference in such a small number of cells. Thus, in addition to vascular dilatation, we observed narrowing of the branchial arch arteries and rostral dorsal aorta in $Ccm1^{-/-}$ embryos at E8.5.

Cardiac development proceeds normally prior to the development of vascular defects

Although vascular defects are first observed at E8.5 and progress with age, we found no evidence of cardiac defects in embryos from E8.0-E9.5. During these stages, mice lacking *Ccm1* completed cardiac looping, developed appropriate endocardial cushions in the AV canal, and showed similar myocardial trabeculation to wild-type embryos (see Fig. S1A-D at http://dev.biologists.org/supplemental/). The expression of the cardiac transcription factors *Hand1* (also known as *eHand*) and *Hand2* (also known as *dHand*), as well as the marker *Nppa* (*natriuretic peptide precursor type A*, also known as *atrial natriuretic factor*) was found to be similar at E8.5 in both wild-type and $Ccm1^{-/-}$ embryos (see Fig. S1E-J at http://dev.biologists.org/supplemental/). As mutant embryos age and begin to suffer from generalized developmental arrest after E9.5, we have frequently observed pericardial effusions and atrial enlargement (data not shown). These studies indicate that vascular defects are the primary defects affecting $Ccm1^{-/-}$ embryos and suggest that cardiac defects observed later in development are secondary.

Neuronal patterning proceeds normally in $Ccm1^{-/-}$ embryos

Concurrent with early vascular development, the embryonic neural tube becomes organized and structured in both anteroposterior (AP) and dorsoventral (DV) aspects as an early step in neural development (Briscoe and Ericson, 2001; Liu and Joyner, 2001). The neural expression of *Ccm1* and the CNS predilection of cavernous malformations led us to investigate neural patterning in $Ccm1^{-/-}$ embryos. In order to determine whether vascular defects occur secondary to neural defects in mice lacking *Ccm1*, we used RNA in situ hybridization to study the AP and DV organization of the developing CNS at E8.5. From anterior to posterior, the CNS at this stage can be divided into the forebrain, midbrain and hindbrain. The hindbrain itself can be subdivided further into 8 rhombomeres (Liu and Joyner, 2001). Molecular markers can also distinguish the midbrain-hindbrain junction, or isthmus, which has an important organizer function (Liu and Joyner, 2001). The homeobox gene *Six3* (Fig. 6A,B) is expressed in the forebrain at E8.5 (Oliver et al., 1995). The transcription factor *Otx2* (Fig. 6C,D) is also expressed in the forebrain and extends into the midbrain up to the isthmus, where expression abruptly stops (Liu and Joyner, 2001). The secreted molecule *Fgf8* (Fig. 6E,F) has a domain of expression restricted to the isthmus at the midbrain-hindbrain junction (Liu and Joyner, 2001). The homeobox gene *Gbx2* (Fig. 6G,H), which helps establish the posterior boundary of the isthmus, is then expressed

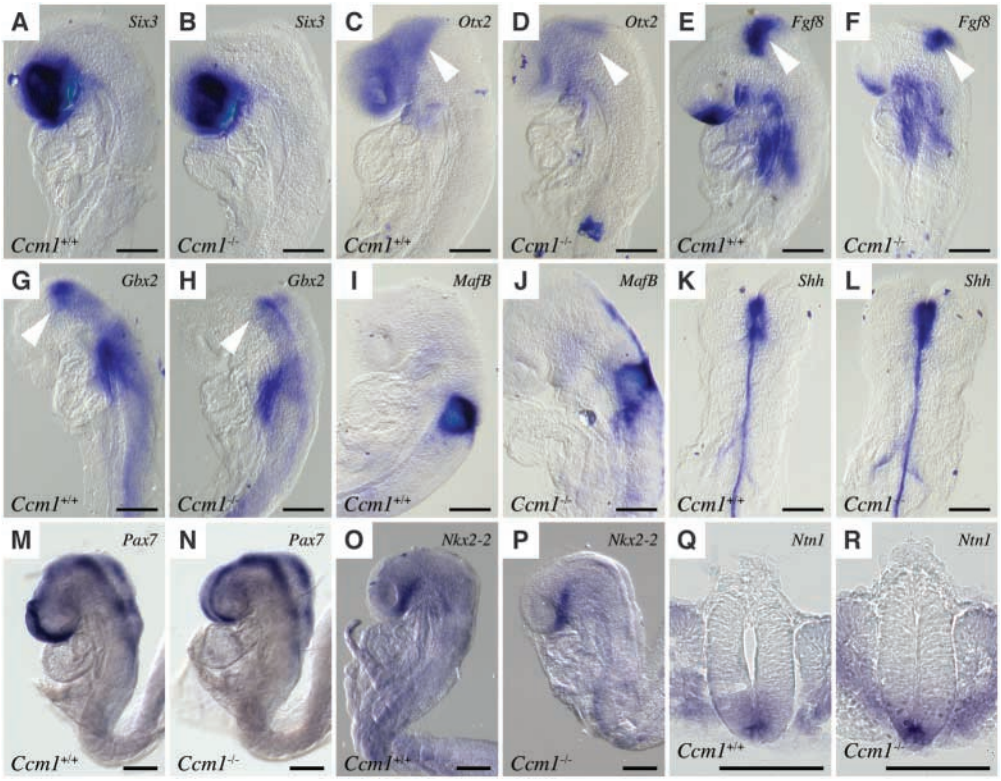

Fig. 6. Neural patterning is not perturbed in *Ccm1*$^{-/-}$ mice. (A-H) In situ hybridization of *Ccm1*$^{+/+}$ and *Ccm1*$^{-/-}$ embryos at E8.5. Arrowheads identify the isthmus between midbrain and hindbrain. (A,B) The expression of the homeobox gene *Six3* is restricted to the forebrain. (C,D) The expression of the transcription factor *Otx2* remains restricted to the forebrain and midbrain in both *Ccm1*$^{+/+}$ and *Ccm1*$^{-/-}$ mice. (E,F) Transcript for *Fgf8* is detected from the isthmus, bounded by the midbrain and hindbrain (arrowheads in all panels). (G,H) The homeobox gene *Gbx2* is expressed throughout the hindbrain, up to the junction with the midbrain (or isthmus) in both wild-type and *Ccm1* homozygous mutant embryos. (I,J) The expression of the leucine zipper transcription factor *MafB* is restricted to rhombomeres 5 and 6 of the hindbrain in both *Ccm1*$^{+/+}$ and *Ccm1*$^{-/-}$ mice. (K,L) The secreted molecule *shh* is expressed in the notochord and ventral floor plate of the neural tube. (M,N) The homeobox gene *Pax7* is expressed along the dorsal neural tube of both genotypes. (O,P) The homeobox gene *Nkx2-2* is expressed in the ventral floor plate of the forebrain at E8.5. (Q,R) The axon guidance molecule *Netrin1* is expressed in the ventral floor plate, as well as in adjacent somites, in *Ccm1*$^{-/-}$ and *Ccm1*$^{+/+}$ mice. All markers studied showed similar expression between *Ccm1*$^{+/+}$ and *Ccm1*$^{-/-}$ mice. Scale bars: 200 μm.

throughout the hindbrain (Liu and Joyner, 2001). Within the hindbrain the leucine zipper transcription factor *MafB* (Fig. 6I,J) is limited in expression to rhombomeres 5 and 6 (Grapin-Botton et al., 1998). Along the AP axis of the neural tube, the secreted protein *Shh* (Fig. 6K,L) is expressed in the notochord and floor plate where it performs an inductive role (Briscoe and Ericson, 2001). The homeobox gene *Pax7* (Fig. 6M,N) is expressed in the dorsal neural tube (Fu et al., 2003; Mansouri et al., 1996). The homeobox gene *Nkx2-2* (Fig. 6O,P) is expressed in the lateral floor plate (Charrier et al., 2002; Fu et al., 2003). The axon guidance molecule *Netrin1* (Fig. 6Q,R) is expressed in the medial floor plate as well as in adjacent somites (Serafini et al., 1996). No alterations in the normal expression pattern of these genes were observed in embryos lacking *Ccm1*. We conclude that AP and DV patterning of the neural tube in *Ccm1*$^{-/-}$ embryos is intact at the onset of vascular defects. These studies indicate that the vascular developmental defects observed in *Ccm1*$^{-/-}$ embryos are not secondary to a primary neural developmental defect.

Impaired arterial identity in *Ccm1*$^{-/-}$ mice

After the initial endothelial tubes form, arteries are distinguished from veins morphologically and by the expression of genetic markers. The establishment of arterial identity is an important early event in angiogenesis, with relevance to vascular defects and malformations (Sorensen et al., 2003; Urness et al., 2000). Starting at around E9.0, vascular smooth muscle cells are recruited by the arterial endothelium (Li et al., 1999). This recruitment occurs at an earlier stage of development in arteries than veins. We analyzed arterial smooth muscle recruitment by immunostaining for alpha smooth muscle actin (α-Sma). At E9.5 α-Sma staining in wild-type embryos is seen in arterial vessels and in cardiac myocytes, but, as expected, is not observed in veins (Fig. 7A). In *Ccm1*$^{-/-}$ embryos, only α-Sma staining of arteries is lost; expression in the heart is maintained (Fig. 7B). Thus, there is a loss of α-Sma staining that is specific to *Ccm1*$^{-/-}$ arteries, indicative of a failure to recruit arterial smooth muscle cells.

Prior to arterial smooth muscle cell recruitment, and prior to the onset of flow (Ji et al., 2003; McGrath et al., 2003), the arterial endothelium is specified and can be distinguished from venous endothelium by genetic markers (Wang et al., 1998). To identify whether *Ccm1*$^{-/-}$ arteries are appropriately specified, we examined the expression of the arterial-specific

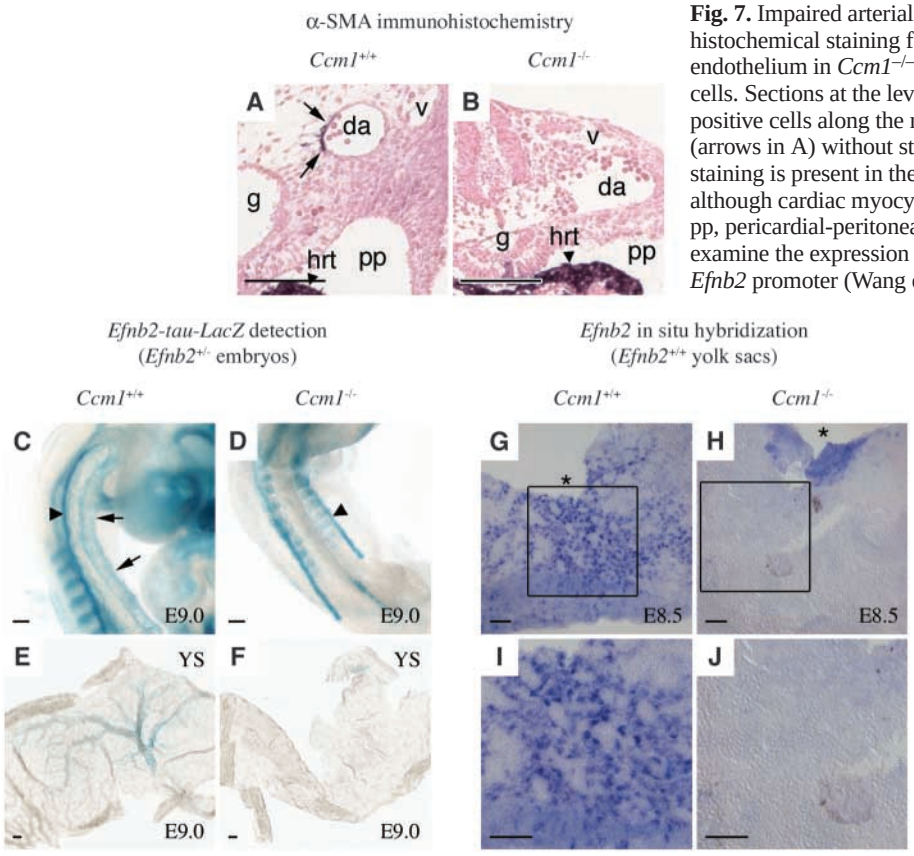

Fig. 7. Impaired arterial identity in mice lacking *Ccm1*. (A,B) Immunohistochemical staining for α-smooth muscle actin shows that the arterial endothelium in *Ccm1*$^{-/-}$ embryos fails to recruit vascular smooth muscle cells. Sections at the level of the atrium of the heart at E9.5 show actin-positive cells along the medial aspect of the wild-type dorsal aorta (arrows in A) without staining of the adjacent cardinal vein. No actin staining is present in the enlarged dorsal aorta of the *Ccm1*$^{-/-}$ embryo (B), although cardiac myocytes stain positive. da, dorsal aorta; v, vein; g, gut; pp, pericardial-peritoneal canal; hrt, heart. (C-F) Staining with X-Gal to examine the expression of a *tau-lacZ* transgene driven by the mouse *Efnb2* promoter (Wang et al., 1998). Embryos shown are all heterozygous for the transgene at the *Efnb2* locus. (C,D) *Efnb2* is expressed in the somites, the nephrogenic cords (arrowheads) and the hindbrain of both genotypes, with arterial expression observed in the dorsal aorta and vitelline artery (arrows, C) of the wild-type embryo. No arterial expression is observed in the *Ccm1*$^{-/-}$ embryo. (E,F) *Efnb2* transgene expression is detected in the yolk sac arteries of a *Ccm1*$^{+/+}$ embryo at E9.0, with no expression observed in the *Ccm1*$^{-/-}$ yolk sac. (G-J) In situ hybridization for *Efnb2* in E8.5 yolk sacs. (G,H) *Efnb2* transcript is detected in the arterial endothelial network of the caudal pole of the yolk sac (asterisks) of a *Ccm1*$^{+/+}$ embryo, with no endothelial stain observed from the same region of a *Ccm1*$^{-/-}$ yolk sac. (I,J) Higher magnification view of yolk sacs (corresponding to boxes in G,H). *Efnb2* stain is observed in individual endothelial cells lining the yolk sac arterial network, with no stain observed in yolk sacs lacking *Ccm1*. Scale bars: 100 μm.

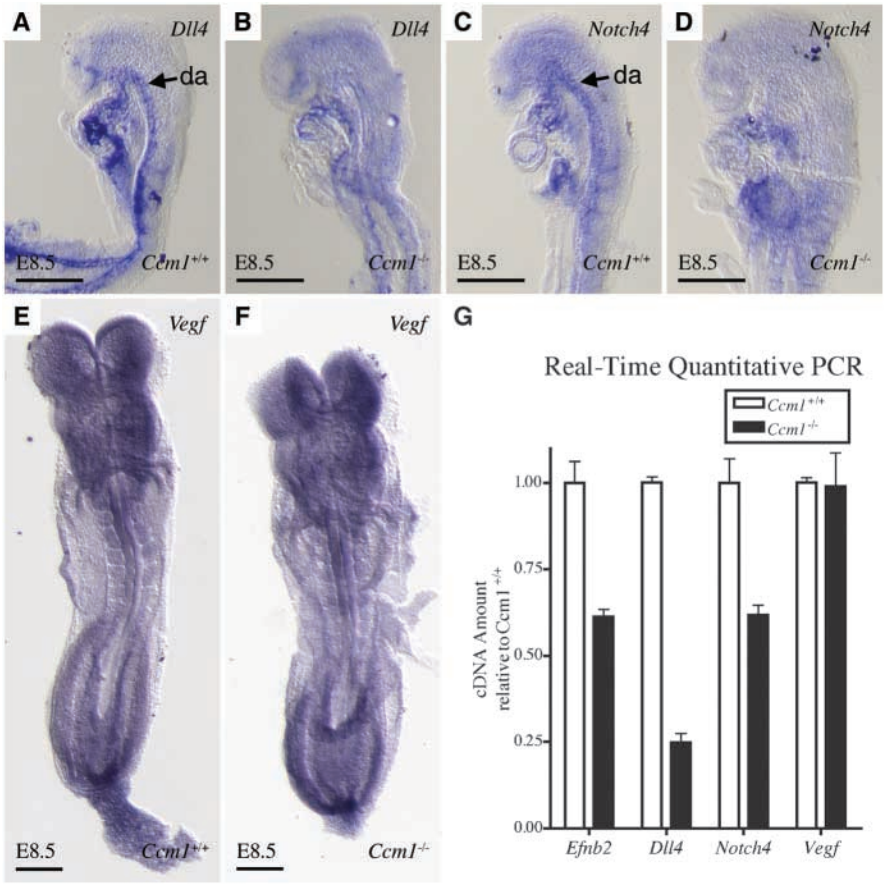

Fig. 8. *Ccm1* lies genetically upstream of *Notch* signaling and downstream of *Vegf*. (A-F) Whole-mount in situ hybridization of *Ccm1*$^{+/+}$ and *Ccm1*$^{-/-}$ tissues at E8.5, before the mutant phenotype can be distinguished grossly. (A-D) Disruption of arterial *Notch* gene expression is demonstrated using probes for *Dll4* and *Notch4*. (A,B) Hybridization with a probe for the *Notch* ligand *Dll4* shows marked downregulation of *Dll4* transcript throughout the dorsal aorta of *Ccm1*$^{-/-}$ embryos, compared with normal controls. (C,D) A decrease in *Notch4* transcript is evident in the branchial arch artery and proximal aorta of a *Ccm1*$^{-/-}$ embryo. The *Notch4* signal intensity was similar, although weak, for the caudal aorta of both the wild type and the mutant. (E,F) In situ hybridization with a probe for *Vegfa* shows a similar intensity of ubiquitous signal from both *Ccm1*$^{+/+}$ and *Ccm1*$^{-/-}$ embryos. (G) Quantification of transcript levels by real-time quantitative PCR at E8.8. Comparison of three pairs of *Ccm1*$^{+/+}$ and *Ccm1*$^{-/-}$ embryo cDNA samples confirmed downregulation of *Efnb2* expression (despite intact extravascular domains of expression shown in Fig. 7A-D). Marked downregulation of *Dll4* with modest downregulation of *Notch4* was also observed, in agreement with the in situ hybridization data. Transcript levels for *Vegfa* were similar between genotypes.

gene *Efnb2* by in situ hybridization, and *Efnb2-tau-lacZ* transgene (Wang et al., 1998) expression by X-Gal staining. Vascular expression of *Efnb2* is downregulated in both the embryo and yolk sac. In the embryo, early *Efnb2* transgene expression is detected in the arterial endothelium, somites, nephrogenic cords and hindbrain. In the absence of *Ccm1*, arterial expression of *Efnb2* is not detected; however, expression in the somites, nephrogenic cord and brain is unaffected (Fig. 7C,D; and data not shown). In the yolk sac, *Efnb2* is expressed only in the endothelium. This is most clearly seen by X-gal staining at E9.0, after the primary plexus has remodeled into an arborizing vascular network. *Efnb2* transgene expression is detected in the arterial vessels of the posterior yolk sac (Fig. 7E). In the absence of *Ccm1*, no staining is observed (Fig. 7F). A similar loss of arterial endothelial expression of *Efnb2* transcript is observed in *Ccm1*$^{-/-}$ yolk sacs before the onset of circulation at E8.5, when the vasculature is composed of a meshwork of homogenously sized endothelial tubes (Fig. 7G-J). The diminished expression of arterial markers and subsequent arterial morphologic defects suggest that arterial identity is impaired in mice lacking *Ccm1*.

Disruption of a pathway governing arterial identity

A genetic pathway has been described in zebrafish placing *Efnb2* expression genetically downstream of *Notch* gene signaling. *Notch* signaling, in turn, is genetically downstream of *Vegfa* in the control of arterial identity (Lawson et al., 2001; Lawson et al., 2002). The expression of the arterial-specific mammalian *Notch* genes, *Dll4* and *Notch4* was significantly downregulated in *Ccm1*$^{-/-}$ embryos by E8.5 (Fig. 8A-D), prior to the gross appearance of the mutant phenotype and prior to the onset of circulation. The expression of the pan-endothelial markers Pecam (Fig. 4A,B) and *Kdr* (data not shown) remained unperturbed. We observed similar intensity and distribution of expression of *Vegfa* (Fig. 8E,F) in *Ccm1*$^{-/-}$ embryos, by in situ hybridization, compared with wild type. The downregulation of arterial markers with intact expression of *Vegfa* in mice lacking *Ccm1* was confirmed and quantified by real-time quantitative RT-PCR (Fig. 8G). These results would suggest that *Ccm1* lies genetically downstream of *Vegf* in the control of *Notch* signaling and arterial morphogenesis.

Downregulation of NOTCH4 in human CCM

Our experiments indicate that arterial identity and development are impaired in *Ccm1*$^{-/-}$ mice. In view of the observed similarities between enlarged vessels in *Ccm1*$^{-/-}$ embryos and human cerebral cavernous malformations, we speculated that a similar disruption of arterial identity (reduced expression of *DLL4*, *NOTCH4* and *EFNB2*) might underlie the pathology in human cavernous malformations. Because antibodies that recognize human EFNB2 and DLL4 are not available, antibodies against human NOTCH4 were used to examine arterial identity in previously excised vascular malformations from three affected individuals of a family with a frameshift mutation (Sahoo et al., 1999) in *CCM1*. Control experiments using autopsy-derived, formalin-fixed brain tissue from unaffected individuals showed prominent and specific expression of NOTCH4 in arterial endothelium and smooth muscle cells (Fig. 9A). In affected individuals, we were not able to detect NOTCH4 expression in cavernous lesions, and there is a marked reduction of NOTCH4 in the arteries of the brain tissue adjacent to the vascular malformation (Fig. 9B). Thus, similar to mice lacking *Ccm1*, humans with loss-of-function mutations in *CCM1* have decreased expression of NOTCH4 in association with vascular malformations.

Discussion

The neural and epithelial expression of *Ccm1* in adulthood had suggested that cavernous malformations might be the result of primary neural defects. In this study we demonstrate an essential role for *Ccm1* in vascular development. The earliest defects in mice lacking *Ccm1* are vascular, and result in thin-walled, endothelial caverns that are reminiscent of human cerebral cavernous malformations. Dilation is observed in the vessels of the cephalic mesenchyme and the dorsal aorta of the caudal embryo, with simultaneous narrowing of the branchial arch arteries and proximal dorsal aorta. No defects in neural patterning or cardiac development are observed prior to the onset of vascular defects. The vascular defects are associated with a loss of arterial endothelial markers (*Efnb2*, *Dll4* and *Notch4*) prior to the onset of flow, and a failure of arterial smooth muscle recruitment to the developing arteries. In human patients, we similarly observe loss of NOTCH4 expression in arteries associated with cerebral cavernous malformations. We conclude from our data that the loss of

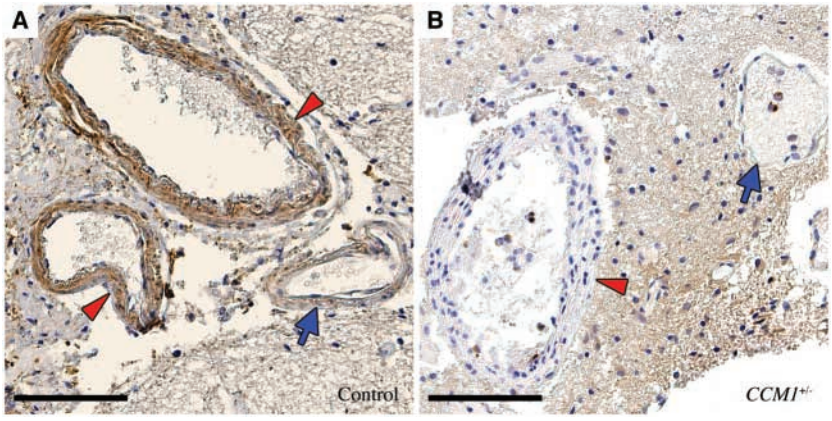

Fig. 9. Downregulation of NOTCH4 in arteries associated with CCM from patients with loss-of-function mutations in *CCM1*. (A,B) Immunohistochemistry using antibodies against NOTCH4 on human tissues. (A) A section of normal brain taken from an autopsy specimen showing NOTCH4 signal from endothelium and vascular smooth muscle cells of two arteries (red arrowheads), without significant expression from an adjacent vein (blue arrow). (B) A section from a surgically excised specimen from a patient with a previously characterized mutation of *CCM1* (Sahoo et al., 1999). An artery (red arrowhead) from brain tissue adjacent to a cavernous malformation shows little NOTCH4 protein in the endothelium or vascular smooth muscle cells. There is no NOTCH4 staining in an adjacent venule (blue arrow). Similar findings were present from two other members of the same family. Scale bars: 100 μm.

Ccm1 leads to primary vascular defects and disrupts the molecular pathway regulating arterial identity.

Role of *Ccm1* in development

Ccm1 is essential for angiogenesis

Vasculogenesis, the de novo formation of endothelial tubes from angioblast precursors (Risau, 1997), is intact in *Ccm1*$^{-/-}$ mice, as the vascular pattern is formed correctly by E8.0. In this study, we demonstrate that *Ccm1* is essential for angiogenesis, the process of vessel maturation and network remodeling wherein new vessels arise from preexisting vessels (Risau, 1997). Mice lacking *Ccm1* die by E11 with prominent vascular defects associated with inappropriate angiogenic remodeling. Arteries in *Ccm1*$^{-/-}$ embryos develop morphologic defects starting at E8.5, with marked enlargement of the caudal aorta and the vessels of the cephalic mesenchyme. We observed increased endothelial proliferation in the dilated aorta of the caudal embryo compared with wild type. This dilatation and proliferation is not a consequence of increased flow as demonstrated by a lack of circulation of India ink when injected into the cardiac ventricle. Narrowing of the branchial arch arteries and the proximal aortae is also present at E8.5. Cardiac development appears entirely normal until E9.5, when generalized developmental arrest occurs in *Ccm1*$^{-/-}$ mice. We conclude that *Ccm1* is required for angiogenesis.

Neural morphology and neural patterning develop normally in mice lacking *Ccm1*

The neural and epithelial expression of *Ccm1* in adulthood suggests that cerebral cavernous vascular malformations may be secondary to neural defects. Our results indicate that loss of *Ccm1* expression results in primary vascular defects in the embryo. Vascular defects in mice lacking *Ccm1* are uniformly present at E8.5. We demonstrate that the anteroposterior and dorsoventral patterning of embryos lacking *Ccm1* is normal at E8.5, based on the expression of a broad panel of genes. The optic and otic anlagen are both present, and no morphologic neural tube defects are observed despite vascular enlargement throughout the embryo. These results suggest that endothelial cells require *Ccm1*. To determine whether *Ccm1* expression is necessary within the endothelial cell itself, or whether endothelial cells depend upon interactions with adjacent cells expressing *Ccm1*, further experiments using conditional mutagenesis will be important.

Ccm1 is required to establish arterial identity

Arteries are distinguished from veins even at the earliest stages of development and prior to the onset of circulation. This distinction is first recognized on the basis of a unique set of molecular markers that label arteries and not veins. We examined the expression of the known arterial markers, *Efnb2*, *Notch4* and *Dll4*, and found significant downregulation of the arterial expression of all three genes by in situ hybridization and by real-time quantitative RT-PCR. The extravascular expression of *Efnb2* from somites, nephrogenic cord and hindbrain remains intact in *Ccm1*$^{-/-}$ embryos, suggesting a specific effect of *Ccm1* on arterial identity. These data demonstrate that arterial specification of endothelial tubes is disrupted in *Ccm1*$^{-/-}$ mice.

Recently, much progress has been made in understanding the process by which arteries are distinguished from veins. This process is best understood in the zebrafish, a model organism particularly well suited to the establishment of genetic pathways (Fishman, 2001). In the zebrafish, loss of Notch signaling leads to a reduction of arterial *Efnb2* expression, and abnormal arterial-venous connections as seen angiographically (Lawson et al., 2001). The expression of *Vegf* was shown to be necessary for Notch signaling and *Efnb2* expression (Lawson et al., 2002). This genetic pathway has not been confirmed in mammalian systems, in part because of the relative difficulty in genetically manipulating mice compared with zebrafish. In our studies, we found no detectable disruption of *Vegf* expression in mice lacking *Ccm1*. These data suggest that *Ccm1* lies genetically downstream of *Vegf*, and indicates that it is genetically upstream of *Notch* and *Efnb2* signaling in the control of arterial specification.

In mammalian systems, it has been demonstrated that *Notch* signaling is important for vascular development (D'Amore and Ng, 2002; Gridley, 2001; Krebs et al., 2000; Leong et al., 2002). The combined loss of the *Notch1* and *Notch4* receptors leads to severe vascular defects including narrowed or collapsed dorsal aortae (Krebs et al., 2000). The vascular defects observed in *Notch1* and *Notch4* double-mutant embryos are more severe than those observed in mice lacking *Notch1* alone, whereas mice lacking *Notch4* show no phenotype (Krebs et al., 2000). These studies have led others to hypothesize that genetic interactions between *Notch4* and *Notch1* are important for angiogenic vascular remodeling (Krebs et al., 2000). Our studies support a crucial role for *Notch* signaling in angiogenesis, and suggest that disruption of *Notch4*, with its probable ligand *Dll4*, may contribute to the vascular phenotype observed in *Ccm1*$^{-/-}$ mice. These studies lead to a hypothesis that is readily tested: whereas disruption of *Notch4* may lead to no phenotype, ablating the endothelial expression of both *Notch4* and *Dll4* in mice will result in a severe vascular phenotype reminiscent of *Ccm1*$^{-/-}$ mice.

Insights into the role of *CCM1* in disease

Impaired arterial identity associated with human cavernous malformations

The disruption of the Notch signaling pathway in *Ccm1*$^{-/-}$ mice led us to postulate that a similar reduction in NOTCH expression may be important in the pathogenesis of human cavernous malformations. Our studies of affected individuals with known mutations in *CCM1* (Marchuk et al., 1995; Sahoo et al., 1999) show that NOTCH4 is significantly reduced in arterioles associated with CCM lesions. We were unable to test the expression of *EFNB2* and *DLL4* because neither reliable antibodies, nor frozen sections for in situ hybridization from these affected individuals are available. We observe additional parallels between the human lesions and mice lacking *Ccm1*. Both exhibit enlarged, thin-walled vessels that lack vascular smooth muscle support. In both instances, the enlarged vessels do not opacify well angiographically, suggesting that human lesions are isolated from a significant arterial supply. We demonstrate that cavernous lesions in mice lacking *Ccm1* are isolated from arterial inflow by vascular narrowing proximal to the lesion. This suggests that similar narrowing may be present in human lesions. The decrease in NOTCH4 and these other parallels lead us to further suggest that impaired arterial specification may contribute to the etiology of CCM.

This characterization of *Ccm1*$^{-/-}$ mice exemplifies the

efficacy of studying vascular malformation genes to better understand arterial development. We have previously characterized mice lacking the two genes known to cause Hereditary Hemorrhagic Telangiectasia, an autosomal dominant vascular dysplasia caused by loss-of-function mutations in either *endoglin* (*Eng*) (Li et al., 1999) or *activin receptor-like kinase 1* (*Acvrl1*) (Urness et al., 2000). Affected individuals develop enlarged arteriovenous channels that bypass capillary beds, and are prone to rupture (Guttmacher et al., 1995). Mice lacking *Acvrl1* and *Eng* fail to maintain distinct arterial and venous beds, developing similar arteriovenous shunts (Sorensen et al., 2003; Urness et al., 2000). These three examples suggest that a natural mutagenesis screen has occurred in humans, in which the readout of vascular malformations suggests disruption of genes involved in arterial and venous development.

We thank L. D. Urness and K. R. Thomas for helpful comments; D. N. Louis for cavernous malformation specimens; J. Lee and L. K. Sorensen for technical assistance; and C. Rodesch from the University of Utah Cell Imaging Core. Embryonic stem cell culture and generation of chimeric mice was performed by the Duke Comprehensive Cancer Center Transgenic Mouse Facility. We would also like to thank C. B. McKinney and the members of the Huntsman Cancer Institute Tissue Access and Tissue Imaging and Analytical Morphology Cores, supported by the Huntsman Cancer Foundation and grants CA2014 and CA73922 from the NIH. This work was supported by grants from the National Institutes of Health and the American Cancer Society, and a Technology Commercialization Grant from the University of Utah. K.J.W. is a Pfizer Postdoctoral Fellow.

References

Arias, E. and Smith, B. L. (2003). Deaths: preliminary data for 2001. *Natl. Vital Stat. Rep.* **51**, 1-44.

Barrow, J. R., Thomas, K. R., Boussadia-Zahui, O., Moore, R., Kemler, R., Capecchi, M. R. and McMahon, A. P. (2003). Ectodermal Wnt3/beta-catenin signaling is required for the establishment and maintenance of the apical ectodermal ridge. *Genes Dev.* **17**, 394-409.

Brenner, R. M., Slayden, O. D., Rodgers, W. H., Critchley, H. O., Carroll, R., Nie, X. J. and Mah, K. (2003). Immunocytochemical assessment of mitotic activity with an antibody to phosphorylated histone H3 in the macaque and human endometrium. *Hum. Reprod.* **18**, 1185-1193.

Briscoe, J. and Ericson, J. (2001). Specification of neuronal fates in the ventral neural tube. *Curr. Opin. Neurobiol.* **11**, 43-49.

Charrier, J. B., Lapointe, F., Le Douarin, N. M. and Teillet, M. A. (2002). Dual origin of the floor plate in the avian embryo. *Development* **129**, 4785-4796.

Craig, H. D., Gunel, M., Cepeda, O., Johnson, E. W., Ptacek, L., Steinberg, G. K., Ogilvy, C. S., Berg, M. J., Crawford, S. C., Scott, R. M. et al. (1998). Multilocus linkage identifies two new loci for a mendelian form of stroke, cerebral cavernous malformation, at 7p15-13 and 3q25.2-27. *Hum. Mol. Genet.* **7**, 1851-1858.

D'Amore, P. A. and Ng, Y. S. (2002). Won't you be my neighbor? Local induction of arteriogenesis. *Cell* **110**, 289-292.

Del Curling, O., Jr, Kelly, D. L., Jr, Elster, A. D. and Craven, T. E. (1991). An analysis of the natural history of cavernous angiomas. *J. Neurosurg.* **75**, 702-708.

Denier, C., Gasc, J., Chapon, F., Domenga, V., Lescoat, C., Joutel, A. and Tournier-Lasserve, E. (2002). Krit1/cerebral cavernous malformation 1 mRNA is preferentially expressed in neurons and epithelial cells in embryo and adult. *Mech. Dev.* **117**, 363.

Drake, C. J. and Fleming, P. A. (2000). Vasculogenesis in the day 6.5 to 9.5 mouse embryo. *Blood* **95**, 1671-1679.

Faisst, A. M. and Gruss, P. (1998). Bodenin: a novel murine gene expressed in restricted areas of the brain. *Dev. Dyn.* **212**, 293-303.

Fishman, M. C. (2001). Genomics. Zebrafish – the canonical vertebrate. *Science* **294**, 1290-1291.

Fu, H., Qi, Y., Tan, M., Cai, J., Hu, X., Liu, Z., Jensen, J. and Qiu, M. (2003). Molecular mapping of the origin of postnatal spinal cord ependymal cells: evidence that adult ependymal cells are derived from Nkx6.1+ ventral neural progenitor cells. *J. Comp. Neurol.* **456**, 237-244.

Grapin-Botton, A., Bonnin, M. A., Sieweke, M. and Le Douarin, N. M. (1998). Defined concentrations of a posteriorizing signal are critical for MafB/Kreisler segmental expression in the hindbrain. *Development* **125**, 1173-1181.

Gridley, T. (2001). Notch signaling during vascular development. *Proc. Natl. Acad. Sci. USA* **98**, 5377-5378.

Gunel, M., Laurans, M. S., Shin, D., DiLuna, M. L., Voorhees, J., Choate, K., Nelson-Williams, C. and Lifton, R. P. (2002). KRIT1, a gene mutated in cerebral cavernous malformation, encodes a microtubule-associated protein. *Proc. Natl. Acad. Sci. USA* **99**, 10677-10682.

Guttmacher, A. E., Marchuk, D. A. and White, R. I., Jr (1995). Hereditary hemorrhagic telangiectasia. *N. Engl. J. Med.* **333**, 918-924.

Hendzel, M. J., Wei, Y., Mancini, M. A., Van Hooser, A., Ranalli, T., Brinkley, B. R., Bazett-Jones, D. P. and Allis, C. D. (1997). Mitosis-specific phosphorylation of histone H3 initiates primarily within pericentromeric heterochromatin during G2 and spreads in an ordered fashion coincident with mitotic chromosome condensation. *Chromosoma* **106**, 348-360.

Ji, R. P., Phoon, C. K., Aristizabal, O., McGrath, K. E., Palis, J. and Turnbull, D. H. (2003). Onset of cardiac function during early mouse embryogenesis coincides with entry of primitive erythroblasts into the embryo proper. *Circ. Res.* **92**, 133-135.

Joutel, A., Corpechot, C., Ducros, A., Vahedi, K., Chabriat, H., Mouton, P., Alamowitch, S., Domenga, V., Cecillion, M., Marechal, E. et al. (1996). Notch3 mutations in CADASIL, a hereditary adult-onset condition causing stroke and dementia. *Nature* **383**, 707-710.

Kehrer-Sawatzki, H., Wilda, M., Braun, V. M., Richter, H. P. and Hameister, H. (2002). Mutation and expression analysis of the KRIT1 gene associated with cerebral cavernous malformations (CCM1). *Acta Neuropathol. (Berl.)* **104**, 231-240.

Krebs, L. T., Xue, Y., Norton, C. R., Shutter, J. R., Maguire, M., Sundberg, J. P., Gallahan, D., Closson, V., Kitajewski, J., Callahan, R. et al. (2000). Notch signaling is essential for vascular morphogenesis in mice. *Genes Dev.* **14**, 1343-1352.

Laberge-le Couteulx, S., Jung, H. H., Labauge, P., Houtteville, J. P., Lescoat, C., Cecillon, M., Marechal, E., Joutel, A., Bach, J. F. and Tournier-Lasserve, E. (1999). Truncating mutations in CCM1, encoding KRIT1, cause hereditary cavernous angiomas. *Nat. Genet.* **23**, 189-193.

Lawson, N. D., Scheer, N., Pham, V. N., Kim, C. H., Chitnis, A. B., Campos-Ortega, J. A. and Weinstein, B. M. (2001). Notch signaling is required for arterial-venous differentiation during embryonic vascular development. *Development* **128**, 3675-3683.

Lawson, N. D., Vogel, A. M. and Weinstein, B. M. (2002). sonic hedgehog and vascular endothelial growth factor act upstream of the Notch pathway during arterial endothelial differentiation. *Dev. Cell* **3**, 127-136.

Leong, K. G., Hu, X., Li, L., Noseda, M., Larrivee, B., Hull, C., Hood, L., Wong, F. and Karsan, A. (2002). Activated Notch4 inhibits angiogenesis: role of beta 1-integrin activation. *Mol. Cell. Biol.* **22**, 2830-2841.

Li, D. Y., Sorensen, L. K., Brooke, B. S., Urness, L. D., Davis, E. C., Taylor, D. G., Boak, B. B. and Wendel, D. P. (1999). Defective angiogenesis in mice lacking endoglin. *Science* **284**, 1534-1537.

Liu, A. and Joyner, A. L. (2001). Early anterior/posterior patterning of the midbrain and cerebellum. *Annu. Rev. Neurosci.* **24**, 869-896.

Lynch, J. K., Hirtz, D. G., DeVeber, G. and Nelson, K. B. (2002). Report of the National Institute of Neurological Disorders and Stroke workshop on perinatal and childhood stroke. *Pediatrics* **109**, 116-123.

Mansouri, A., Stoykova, A., Torres, M. and Gruss, P. (1996). Dysgenesis of cephalic neural crest derivatives in Pax7–/– mutant mice. *Development* **122**, 831-838.

Marchuk, D. A., Gallione, C. J., Morrison, L. A., Clericuzio, C. L., Hart, B. L., Kosofsky, B. E., Louis, D. N., Gusella, J. F., Davis, L. E. and Prenger, V. L. (1995). A locus for cerebral cavernous malformations maps to chromosome 7q in two families. *Genomics* **28**, 311-314.

McGrath, K. E., Koniski, A. D., Malik, J. and Palis, J. (2003). Circulation is established in a stepwise pattern in the mammalian embryo. *Blood* **101**, 1669-1676.

Moriarity, J. L., Clatterbuck, R. E. and Rigamonti, D. (1999). The natural history of cavernous malformations. *Neurosurg. Clin. N. Am.* **10**, 411-417.

Nechiporuk, A. and Keating, M. T. (2002). A proliferation gradient between proximal and msxb-expressing distal blastema directs zebrafish fin regeneration. *Development* **129**, 2607-2617.

Oliver, G., Mailhos, A., Wehr, R., Copeland, N. G., Jenkins, N. A. and Gruss, P. (1995). Six3, a murine homologue of the sine oculis gene, demarcates the most anterior border of the developing neural plate and is expressed during eye development. *Development* **121**, 4045-4055.

Otten, P., Pizzolato, G. P., Rilliet, B. and Berney, J. (1989). A propos de 131 cas d'angiomes caverneux (cavernomes) du S.N.C. repérés par l'analyse rétrospective de 24 535 autopsies. *Neurochirurgie* **35**, 128-131.

Park, K. W., Morrison, C. M., Sorensen, L. K., Jones, C. A., Rao, Y., Chien, C. B., Wu, J. Y., Urness, L. D. and Li, D. Y. (2003). Robo4 is a vascular-specific receptor that inhibits endothelial migration. *Dev. Biol.* **261**, 251-267.

Rigamonti, D., Hadley, M. N., Drayer, B. P., Johnson, P. C., Hoenig-Rigamonti, K., Knight, J. T. and Spetzler, R. F. (1988). Cerebral cavernous malformations. Incidence and familial occurrence. *N. Engl. J. Med.* **319**, 343-347.

Risau, W. (1997). Mechanisms of angiogenesis. *Nature* **386**, 671-674.

Robinson, J. R., Awad, I. A. and Little, J. R. (1991). Natural history of the cavernous angioma. *J. Neurosurg.* **75**, 709-714.

Robinson, J. R., Jr, Awad, I. A., Masaryk, T. J. and Estes, M. L. (1993). Pathological heterogeneity of angiographically occult vascular malformations of the brain. *Neurosurgery* **33**, 547-554.

Ruhrberg, C., Gerhardt, H., Golding, M., Watson, R., Ioannidou, S., Fujisawa, H., Betsholtz, C. and Shima, D. T. (2002). Spatially restricted patterning cues provided by heparin-binding VEGF-A control blood vessel branching morphogenesis. *Genes Dev.* **16**, 2684-2698.

Sahoo, T., Johnson, E. W., Thomas, J. W., Kuehl, P. M., Jones, T. L., Dokken, C. G., Touchman, J. W., Gallione, C. J., Lee-Lin, S. Q., Kosofsky, B. et al. (1999). Mutations in the gene encoding KRIT1, a Krev-1/rap1a binding protein, cause cerebral cavernous malformations (CCM1). *Hum. Mol. Genet.* **8**, 2325-2333.

Sahoo, T., Goenaga-Diaz, E., Serebriiskii, I. G., Thomas, J. W., Kotova, E., Cuellar, J. G., Peloquin, J. M., Golemis, E., Beitinjaneh, F., Green, E. D. et al. (2001). Computational and experimental analyses reveal previously undetected coding exons of the KRIT1 (CCM1) gene. *Genomics* **71**, 123-126.

Serafini, T., Colamarino, S. A., Leonardo, E. D., Wang, H., Beddington, R., Skarnes, W. C. and Tessier-Lavigne, M. (1996). Netrin-1 is required for commissural axon guidance in the developing vertebrate nervous system. *Cell* **87**, 1001-1014.

Serebriiskii, I., Estojak, J., Sonoda, G., Testa, J. R. and Golemis, E. A. (1997). Association of Krev-1/rap1a with Krit1, a novel ankyrin repeat-containing protein encoded by a gene mapping to 7q21-22. *Oncogene* **15**, 1043-1049.

Sorensen, L. K., Brooke, B. S., Li, D. Y. and Urness, L. D. (2003). Loss of distinct arterial and venous boundaries in mice lacking endoglin, a vascular-specific TGFbeta coreceptor. *Dev. Biol.* **261**, 235-250.

Tybulewicz, V. L., Crawford, C. E., Jackson, P. K., Bronson, R. T. and Mulligan, R. C. (1991). Neonatal lethality and lymphopenia in mice with a homozygous disruption of the c-abl proto-oncogene. *Cell* **65**, 1153-1163.

Urness, L. D., Sorensen, L. K. and Li, D. Y. (2000). Arteriovenous malformations in mice lacking activin receptor-like kinase-1. *Nat. Genet.* **26**, 328-331.

Wang, H. U., Chen, Z. F. and Anderson, D. J. (1998). Molecular distinction and angiogenic interaction between embryonic arteries and veins revealed by ephrin-B2 and its receptor Eph-B4. *Cell* **93**, 741-753.

Zawistowski, J. S., Serebriiskii, I. G., Lee, M. F., Golemis, E. A. and Marchuk, D. A. (2002). KRIT1 association with the integrin-binding protein ICAP-1: a new direction in the elucidation of cerebral cavernous malformations (CCM1) pathogenesis. *Hum. Mol. Genet.* **11**, 389-396.

Zhang, J., Clatterbuck, R. E., Rigamonti, D. and Dietz, H. C. (2000). Cloning of the murine Krit1 cDNA reveals novel mammalian 5′ coding exons. *Genomics* **70**, 392-395.

Zhang, J., Clatterbuck, R. E., Rigamonti, D., Chang, D. D. and Dietz, H. C. (2001). Interaction between krit1 and icap1alpha infers perturbation of integrin beta1-mediated angiogenesis in the pathogenesis of cerebral cavernous malformation. *Hum. Mol. Genet.* **10**, 2953-2960.